Uncoupled matching for active and passive impedances of coupled arrays in MIMO systems

Jensen, Michael Allen; Lau, Buon Kiong

Published in:
IEEE Transactions on Antennas and Propagation

DOI:
10.1109/TAP.2010.2055803

2010

Document Version:
Peer reviewed version (aka post-print)

Uncoupled Matching for Active and Passive Impedances of Coupled Arrays in MIMO Systems

Michael A. Jensen, *Fellow, IEEE* and Buon Kiong Lau, *Senior Member, IEEE*

***Abstract*—Impedance matching for coupled antenna arrays has received considerable attention in the research community. Because optimal matching requires implementation of a coupled network, leading to high complexity and often narrow operation bandwidth, new research has focused on the development of uncoupled matching networks with good performance. This paper explores traditional uncoupled impedance matching techniques for coupled arrays, specifically matching to the array *active* and *passive* impedances, within the context of multiple-input multiple-output communication. The concept of matching to the array active impedance is extended to the case where the propagating field is specified stochastically, and the performance of this solution is compared to that of traditional solutions using simulations. While emphasis is placed on matching for maximum power transfer, the paper concludes with a discussion on matching for minimum amplifier noise figure.**

***Index Terms*—Antenna array mutual coupling, Impedance matching, MIMO systems**

I. Introduction

CURRENT INTEREST in using multi-antenna technology to enhance wireless communication performance coupled with the small antenna separation mandated by compact mobile devices have led to vigorous interest in impedance matching techniques that compensate for the degradation created by antenna mutual coupling. Optimal solutions to this problem require coupled matching networks, with examples being the well-known optimal multiport conjugate match (MCM) for maximum power transfer [1]–[3] and the corresponding result for minimum noise figure [4]–[6]. Unfortunately, such coupled networks are typically complicated and often result in narrowband matching performance [7].

The challenges associated with implementation of optimal matching motivate the identification of uncoupled matching networks that achieve near-optimal performance. In traditional array research, this is typically accomplished by matching to the array self, *passive* [8], [9], or *active* [10] impedance. However, when it comes to multiple-input multiple-output (MIMO) systems, where the objectives of the array processing generally differ from those for traditional or beamforming arrays, the exploration of these uncoupled matching techniques has been limited, with most work considering either numerically-optimized solutions for a given open-circuit covariance [11], [12] or *input impedance matching* [7], which respectively represent forms of matching to the active and passive impedances. In this MIMO context, therefore, we lack a common theoretical framework for designing such networks, a detailed understanding of their different behaviors, and a careful comparison of their relative performance.

This paper focuses on uncoupled matching for MIMO systems by formulating these solutions under a common theoretical framework and discussing each approach in the context of what is known about the propagation channel. Furthermore, because the channel is typically time-variant, we demonstrate how to extend the concept of matching to the active array impedance to the case of stochastically-specified fields. The ergodic channel capacity achieved with these matching techniques is compared to that resulting from a numerically-optimized impedance match. Simulations with closed-form and numerically-generated antenna characteristics illustrate that active impedance matching provides good beamforming gain and optimal MIMO capacity for small signal-to-noise ratio (SNR) or high antenna coupling, while passive matching achieves superior performance for high SNR and low coupling. While the paper focuses on matching for maximum power transfer, it concludes with an approach for applying the methods to achieve minimum amplifier noise figure.

II. Matching for Power Transfer

A common design goal is to maximize the power transferred either from the transmit power amplifiers to the antennas or from the receiving antennas to the terminating loads. The goal of this section is therefore to formulate the uncoupled terminations that achieve this maximum power transfer. Throughout this analysis, boldface lowercase and uppercase symbols denote vectors and matrices respectively, while script versions of the symbols indicate elements of the vector or matrix (v_m is the mth element of the vector $\mathbf{v}$). An overbar indicates a vector electromagnetic quantity.

Let the mth antenna in an M-element array be characterized by an open-circuit radiation pattern (pattern with all other elements terminated in an open circuit) denoted as $\overline{E}_m(\Omega)$, where $\Omega = (\theta, \phi)$ with θ and ϕ representing the elevation and azimuth angles in a spherical coordinate frame, as shown in Fig. 1. If the electric field incident on the array is $\overline{E}_{\rm inc}(\Omega)$, the open-circuit voltage $v_{o,m}$ on this antenna is given as

$$v_{o,m} = \int_{\Omega} \overline{E}_m(\Omega) \cdot \overline{E}_{\rm inc}(\Omega)\, d\Omega. \tag{1}$$

This work was supported in part by Telefonaktiebolaget LM Ericssons Stiftelse för Främjande av Elektroteknisk Forskning, Vetenskapsrådet under Grant 2006–3012, and in part by the U. S. Army Research Office under the Multi-University Research Initiative (MURI) Grants # W911NF-04-1-0224 and # W911NF-07-1-0318.

M. A. Jensen is with the Electrical and Computer Engineering Department, Brigham Young University, Provo, UT 84602, TEL: (801) 422-5349, FAX: (801) 422-0201, email: jensen@ee.byu.edu

B. K. Lau is with the Department of Electrical and Information Technology, Lund University, Box 118, SE-221 00 Lund. Sweden, email: bkl@eit.lth.se

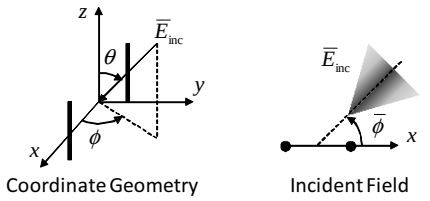

Fig. 1. Geometry showing a two-element z-oriented dipole array and the incident electric field in the system coordinate frame.

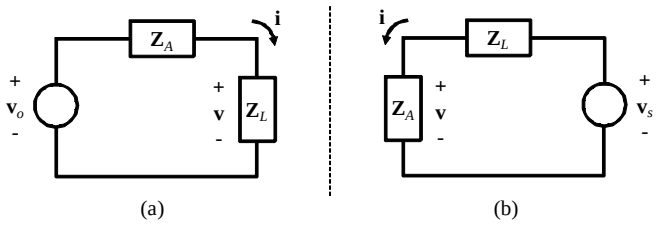

Fig. 2. Impedance parameter equivalent network model of a coupled antenna array at the (a) receiver and (b) transmitter.

If the array is further characterized by a full impedance matrix $\mathbf{Z}_A$ and is terminated in a load having an impedance matrix $\mathbf{Z}_L$, then the equivalent circuit for the receiving system is that shown in Fig. 2(a) [13]. In this network, $\mathbf{v}$ and $\mathbf{i}$ respectively represent the voltage across and the current through the termination. It has been well-established that maximum power is transferred to the load for the MCM [3], or $\mathbf{Z}_L = \mathbf{Z}_A^\dagger$, where $\{\cdot\}^\dagger$ indicates a conjugate transpose. This requires a coupled termination (or matching network), which typically leads to implementation complexity and reduced bandwidth [7].

A. Deterministic Field Matching: Active Impedance

Maintaining maximum power transfer while avoiding the complexities associated with the MCM is possible for a specific incident field (or equivalently value of $\mathbf{v}_o$) using the notion of matching to the array active impedance, the goal of which is to maintain the voltages and currents associated with the optimally-terminated network [6], [10]. This is accomplished through the relations

$$\mathbf{Z}_L\mathbf{i} = \mathbf{Z}_A^\dagger\mathbf{i} = \mathbf{Z}_{\text{act}}^*\mathbf{i} \quad (2)$$

$$\mathbf{v}_o = (\mathbf{Z}_L + \mathbf{Z}_A)\mathbf{i}, \quad (3)$$

where $\mathbf{Z}_{\text{act}}$ is the active impedance, $\mathbf{Z}_L$ and $\mathbf{Z}_{\text{act}}$ are diagonal matrices, and $\{\cdot\}^*$ is the conjugate. Using (2) in (3) leads to $\mathbf{v}_o = (\mathbf{Z}_A^\dagger + \mathbf{Z}_A)\mathbf{i} = \mathbf{Z}_B\mathbf{i}$, where $\mathbf{Z}_B = (\mathbf{Z}_A^\dagger + \mathbf{Z}_A)$. Note that $\mathbf{Z}_B = 2\mathbf{R}_A$, with $\mathbf{R}_A$ being the real part of $\mathbf{Z}_A$, under the assumption of reciprocal antennas that satisfy $\mathbf{Z}_A = \mathbf{Z}_A^T$, where $\{\cdot\}^T$ is the transpose. Solving this relationship for $\mathbf{i}$ and substituting the result into (2) leads to

$$Z_{L,m} = \frac{\left[\mathbf{Z}_A^\dagger\mathbf{Z}_B^{-1}\mathbf{v}_o\right]_m}{\left[\mathbf{Z}_B^{-1}\mathbf{v}_o\right]_m}, \quad (4)$$

where $[\cdot]_m$ is the mth element of the vector inside the brackets.

B. Stochastic Field Matching

Achieving optimal power transfer for a specific incident field is only practical if the termination can adapt to the changing incident field. When this is infeasible, it is useful to consider the termination that functions over a range of incident field profiles. Consider a discrete set of P incident fields, with the pth field generating the open-circuit voltage $\mathbf{v}_o^{(p)}$ and current $\mathbf{i}^{(p)}$. Finding the load impedance that on average matches the active impedances associated with all excitations means finding the solution minimizing the objective function

$$\gamma_z = \frac{1}{P}\sum_{p=1}^{P}\sum_{m=1}^{M}\left|Z_{L,m}i_m^{(p)} - Z_{\text{act},m}^{(p)*}i_m^{(p)}\right|^2, \quad (5)$$

where $Z_{\text{act},m}^{(p)}$ is the active impedance for the pth excitation. Setting the derivative of (5) with respect to $Z_{L,m}^*$ equal to zero and solving (with the help of (2) and (3)) leads to

$$Z_{L,m} = \frac{\left[\mathbf{Z}_A^\dagger\mathbf{U}\right]_{mm}}{U_{mm}} \quad (6)$$

$$\mathbf{U} = \mathbf{Y}\underbrace{\frac{1}{P}\sum_{p=1}^{P}\mathbf{v}_o^{(p)}\mathbf{v}_o^{(p)\dagger}}_{\mathbf{K}_o}\mathbf{Y}^\dagger, \quad (7)$$

where $\mathbf{Y} = (\mathbf{Z}_L + \mathbf{Z}_A)^{-1}$ and $[\cdot]_{mn}$ denotes the mnth element of the matrix inside the brackets.

Since $\mathbf{Z}_L$ appears within $\mathbf{U}$, we solve (6) by first initializing the load impedance (for example, $Z_{L,m} = Z_{A,mm}^*$) and then constructing $\mathbf{Y}$ and $\mathbf{U}$ using (7). We compute $\mathbf{Z}_L$ using (6), and use this new value to update $\mathbf{Y}$ and $\mathbf{U}$. This procedure repeats iteratively until it achieves convergence.

In the limit as $P \to \infty$, the sum in (7) becomes a true expectation over the stochastic set of excitations. We assume that the fields are zero-mean Gaussian random processes obeying the angular correlation model

$$\mathrm{E}\left\{\overline{E}_{\text{inc}}(\Omega)\overline{E}_{\text{inc}}^\dagger(\Omega')\right\} = \overline{\overline{S}}(\Omega)\delta(\Omega - \Omega'), \quad (8)$$

where $\overline{\overline{S}}(\Omega) = \mathrm{E}\left\{\overline{E}_{\text{inc}}(\Omega)\overline{E}_{\text{inc}}^\dagger(\Omega)\right\}$ is the dyadic power angular spectrum (PAS) of the incident field and $\mathrm{E}\{\cdot\}$ denotes the expectation. Substitution of (1) into the expression for $\mathbf{K}_o$ shown in (7) yields the covariance of $\mathbf{v}_o$ given as [14]

$$K_{o,mn} = \int_\Omega \overline{E}_m(\Omega)\cdot\overline{\overline{S}}(\Omega)\cdot\overline{E}_n^*(\Omega)\,d\Omega. \quad (9)$$

C. Unknown Field Matching

Systems often operate in a variety of scenarios, making it impossible to impedance match even to the stochastic nature of the fields. If the system cannot adapt its termination to changing statistics, then the termination should be designed to accommodate all incident fields. One simple approach is to set $\overline{\overline{S}}(\Omega) = 1/4\pi$ in (9) (field arriving from all angles) and use this PAS to design the matching network. In this scenario, $\mathbf{K}_o \propto \mathbf{R}_A$, which is the mutual resistance of the coupled array [6], [15]. Since any difference in scaling is removed in (6), we can use $\mathbf{U} = \mathbf{Y}\mathbf{R}_A\mathbf{Y}^\dagger$.

An alternate approach is to match to the array passive impedance [8], [9], which is the input impedance seen looking into each antenna port. While a closed-form derivation of the terminations that allow all ports to be simultaneously matched to their input impedances is simple for the case of two identical antennas [7], [16], the solution becomes tedious for larger or inhomogeneous arrays. Therefore, consider the antenna array used in transmit mode as depicted in Fig. 2(b) for which $\mathbf{i} = \mathbf{Y}\mathbf{v}_s$ and $\mathbf{v} = \mathbf{Z}_A\mathbf{i}$. We excite the array with a voltage v_s on the mth port and zero voltage on the other ports and subsequently compute the input impedance seen looking into the coupled array from the mth port. The load impedance for this port is then chosen as the conjugate of this input impedance, which can be expressed as

$$Z_{L,m} = \left\{ \frac{[\mathbf{Z}_A\mathbf{Y}]_{mm}}{Y_{mm}} \right\}^* . \tag{10}$$

Since $\mathbf{Z}_L$ appears in the expression for $\mathbf{Y}$, this equation can be solved iteratively using the procedure outlined in Section II-B.

Fundamentally, the passive impedance represents a special case of the active impedance. Specifically, matching to the active impedance maximizes the received power for a specific beamformer [6]. The passive impedance is the active impedance when the beamformer has only one non-zero weight (i.e. processes the signal from only one antenna port).

D. Superdirective Solutions

The concept of selecting a termination based on the incident field characteristics emphasizes that the uncoupled termination itself serves as a beamformer. As a result, for closely-spaced antennas the terminations may produce superdirective behavior [17], and therefore we should take measures to remove these solutions when designing practical systems.

To assess the level of superdirectivity caused by a termination, we compute the array Q-factor defined as $Q = \mathbf{i}^\dagger\mathbf{i}/\mathbf{i}^\dagger\mathbf{A}\mathbf{i}$, where $\mathbf{A} = \mathbf{R}_A/R_{A,11}$ [18]. This equation is suitable when considering the active impedance match for a specific field. However, when considering stochastic fields, we likely wish to take the average of this quantity, which is difficult given its rational form. However, we may approximate the average Q-factor by taking the ratio of averages. Specifically, using that $\mathbf{i} = \mathbf{Y}\mathbf{v}_o$ and that, as discussed in connection with (7) and (9), $\mathbf{K}_o = \mathrm{E}\left\{\mathbf{v}_o\mathbf{v}_o^\dagger\right\}$, this approximate average Q-factor can be expressed as

$$Q_\mathrm{e} = \frac{\mathrm{E}\left\{\mathbf{v}_o^\dagger\mathbf{Y}^\dagger\mathbf{Y}\mathbf{v}_o\right\}}{\mathrm{E}\left\{\mathbf{v}_o^\dagger\mathbf{Y}^\dagger\mathbf{A}\mathbf{Y}\mathbf{v}_o\right\}} = \frac{\mathrm{Tr}\left[\mathbf{Y}^\dagger\mathbf{Y}\mathbf{K}_o\right]}{\mathrm{Tr}\left[\mathbf{Y}^\dagger\mathbf{A}\mathbf{Y}\mathbf{K}_o\right]}, \tag{11}$$

where $\mathrm{Tr}\left[\cdot\right]$ is the trace.

We also need to limit the allowable superdirectivity in the solution, and we therefore adopt the pragmatic approach of incorporating antenna loss and spatially-white noise in the model [19]. Specifically, if the mth radiating element has a radiation efficiency $e_{\mathrm{A},m}$, then its associated self-impedance $Z_{A,mm}$ can be modified to have resistance $\widehat{R}_{A,mm} = R_{A,mm}/e_{\mathrm{A},m}$. Similarly, the open-circuit covariance matrix should contain the spatially-white noise generated by the antenna loss. For simplicity, we assume that the ratio of the open-circuit noise to open-circuit signal squared voltages is proportional to the ratio of the loss to the radiation resistances, leading to the regularization $\widehat{K}_{o,mm} = K_{o,mm}/e_{\mathrm{A},m}$.

E. S-Parameter Analysis

The developments detailed in this section can be formulated using the full S-parameter matrix of the antenna and the uncoupled reflection coefficient matrix representing the load. For matching to the active impedance given a deterministic field or to the passive impedance as discussed in Sections II-A and II-C, the solutions based on Z-parameters and S-parameters are identical. However, when trying to simultaneously match to a range of active impedances by minimizing the cost function in (5), the relative weight of each term in the cost function for Z-parameters differs from that for S-parameters because of their nonlinear mathematical relationship, and therefore slight differences can occur in the two sets of solutions. In the cases considered in this paper, these slight differences change neither the behavioral trends nor the fundamental conclusions drawn from the results. Furthermore, while the derivation of the corresponding techniques using S-parameters is straightforward, their inclusion requires definition of new notation and terminology. Motivated by these observations and for the sake of conciseness, we therefore forego S-parameter analysis in this paper.

III. Computational Results

A. MIMO System Capacity

While impedance matching for maximum power transfer is applicable to many scenarios, our focus is on comparing the different terminations in terms of MIMO capacity. Let $\mathbf{H}_o$ represent the $M \times M$ transimpedance transfer matrix, or

$$\mathbf{v}_o = \mathbf{H}_o\mathbf{i}_T + \boldsymbol{\eta}_o, \tag{12}$$

where $\mathbf{i}_T$ is the vector of transmit currents and $\boldsymbol{\eta}_o$ is the receiver noise referred to the open-circuit antenna terminals. The instantaneous signal power received by the loads is

$$p_L = \mathbf{i}^\dagger\mathbf{R}_L\mathbf{i} = \mathbf{i}_T^\dagger\mathbf{H}_o^\dagger\mathbf{Y}^\dagger\mathbf{R}_L\mathbf{Y}\mathbf{H}_o\mathbf{i}_T, \tag{13}$$

where $\mathbf{R}_L$ is the diagonal matrix of load resistances. We assume that the transmit array has large element spacing (no coupling, no correlation) so that the transmit currents have the covariance $\mathbf{K}_T = \mathrm{E}\left\{\mathbf{i}_T\mathbf{i}_T^\dagger\right\} = P_T/M\mathbf{I}$, where $\mathbf{I}$ is the identity matrix. We note that $\mathrm{Tr}\left[\mathbf{K}_T\right] = P_T$.

Given an effective channel matrix $\mathbf{H}$ relating the transmit currents to the signals at the loads, the capacity is given by

$$C = \log_2\left|\mathbf{I} + \frac{P_T}{M\sigma_\eta^2}\mathbf{H}\mathbf{H}^\dagger\right|, \tag{14}$$

where σ_η^2 is the noise variance at each load and $|\cdot|$ is the determinant. Since the last term in the determinant represents received SNR, comparison with (13) indicates that

$$\mathbf{H} = \mathbf{R}_L^{1/2}\mathbf{Y}\mathbf{H}_o. \tag{15}$$

This formulation allows us to express the average power received in the loads as $P_L = \mathrm{E}\left\{p_L\right\} = \mathrm{Tr}\left[\mathbf{H}\mathbf{K}_T\mathbf{H}^\dagger\right]$. For all

computational examples, we present the ergodic capacity $C_{\rm e}$ computed as an average over 250 random channel realizations normalized by the average capacity $C_{\rm S}$ for single transmit and receive antennas in the same environment.

B. Channel Matrix and Spatial Covariance

To construct the channel matrix for the simulations, we first realize an $M \times M$ matrix $\mathbf{H}_{\rm w}$ whose entries are independent zero-mean unit-variance complex Gaussian random variables. Using our assumption of uncorrelated transmit signals outlined in Section III-A and assuming that the signals at the receive array have the covariance given by (9), we can use the well-known Kronecker model for the covariance to write $\mathbf{H}_o = \mathbf{K}_o^{1/2}\mathbf{H}_{\rm w}$. This model is known to have deficiencies for small element separation or large arrays [20], but since our goal is to compare the *relative* performance of different terminations, its use here is reasonable.

The normalization used for $\mathbf{H}$ must preserve the impact of element spacing and load impedance on the capacity. To accomplish this, we first construct $\mathbf{H}$ in (15) assuming an infinite antenna separation ($\mathbf{Z}_A$ is diagonal) and with $\mathbf{Z}_L = \mathbf{Z}_A^*$. We then normalize $\mathbf{H}_o$ (or $\mathbf{K}_o$) so that the Frobenius norm of $\mathbf{H}$ is $\|\mathbf{H}\|_F = M$, meaning that P_T/σ_η^2 is the single-input single-output (SISO) SNR as detailed in [16]. We finally construct $\mathbf{H}$ for different terminations $\mathbf{Z}_L$ using this normalized version of $\mathbf{H}_o$ with an antenna efficiency of $e_{{\rm A},m} = 0.97$.

In evaluating the performance of MIMO systems, it is also useful to understand the correlation structure of the signals across the loads. Given our formulation for the capacity and channel matrix, this signal is $\mathbf{s}_L = \mathbf{H}\mathbf{i}_T$ such that (13) becomes $p_L = \mathbf{s}_L^\dagger \mathbf{s}_L$. Since the structure of $\mathbf{H}_o$ leads to $\mathrm{E}\left\{\mathbf{H}_o\mathbf{H}_o^\dagger\right\} = M\mathbf{K}_o$, the covariance of $\mathbf{s}_L$ is given as

$$\mathrm{E}\left\{\mathbf{s}_L\mathbf{s}_L^\dagger\right\} = M\underbrace{\mathbf{R}_L^{1/2}\mathbf{Y}\mathbf{K}_o\mathbf{Y}^\dagger\mathbf{R}_L^{(1/2)T}}_{\mathbf{K}_{\rm s}}. \qquad (16)$$

The properly-normalized off-diagonal elements of this matrix represent the commonly-used correlation coefficients between antennas. However, for this study, we instead use the eigenvalues of this covariance, as this directly translates the correlation into the average power for each of the communication modes. This can be explicitly seen in the upper bound on the ergodic capacity that is computed as [16]

$$C_{\rm e} \le \sum_{m=1}^{M}\left(1 + \frac{P_T}{\sigma_\eta^2}\lambda_m\right), \qquad (17)$$

where λ_m is the mth eigenvalue of $\mathbf{K}_{\rm s}$.

C. Simulation Scenarios

In the computations, the PAS is described by a truncated Gaussian function in elevation centered at $\theta = 90^\circ$ and with an angle spread of 10°. The distribution in azimuth is described either as a constant (uniform distribution) or as a single cluster represented by a truncated Laplacian function with an angle spread of 40° and centered at the angle $\phi = \bar{\phi}$. These PAS functions are computed using the methods in [21]. We use arrays of half-wavelength dipole antennas oriented in the z-direction as shown in Fig. 1, so that these PAS functions represent the average power in the $\hat{\theta}$ polarization.

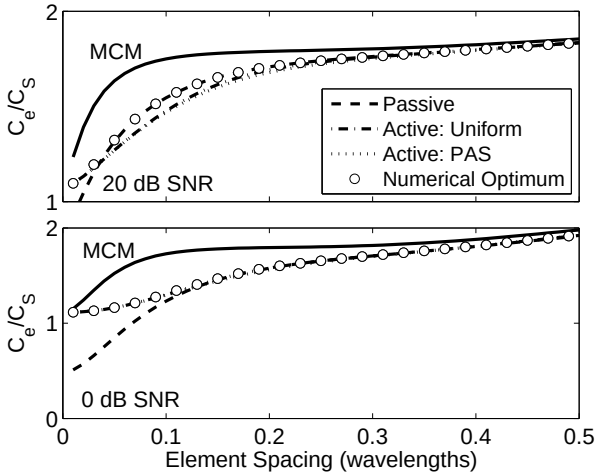

Fig. 3. Normalized average capacity as a function of element spacing for a PAS described by a single Laplacian cluster arriving on a two-element array at broadside for different matching conditions and two different SNR levels.

In all of the cases considered, we first compute the terminations for each of the closed-form techniques (match to the active impedance for the PAS, match to the passive impedance, etc.). We then choose the termination achieving the largest average capacity $C_{\rm e}$ as a seed for a numerical optimization whose goal is to find the uncoupled termination that maximizes this average capacity. Since, however, the capacity as a function of the terminations has local maxima, we generate 250 different starting points by randomly varying the real and imaginary parts of the seed termination uniformly over a range of $\pm 25\%$. For each of these starting points, we complete a Nelder-Mead simplex optimization that determines the termination achieving the local maximum average capacity. Because each of these local maxima potentially represents a unique value of $C_{\rm e}$, the termination achieving the largest value of $C_{\rm e}$ is selected as the optimization outcome.

D. Two-Element Dipole Array

As a starting point in our analysis, we assume a linear array of two half-wave dipole antennas at the receiver. The open-circuit radiation patterns are assumed to be identical to the isolated dipole element patterns computed using the simple formula in [22]. The impedance matrix is also computed using the closed-form expressions in [22]. While this antenna characterization approach is approximate, it provides maximum flexibility in sweeping antenna parameters and therefore allows us to explore basic behaviors before adding the complexity associated with numerical antenna characterization.

Figure 3 plots the capacity as a function of the element spacing for the Laplacian PAS at $\bar{\phi} = 90^\circ$ (broadside) using the different terminations and for two different values of the SISO SNR. The performance for a perfect MCM is shown for comparison. Figure 4 plots the same results when the

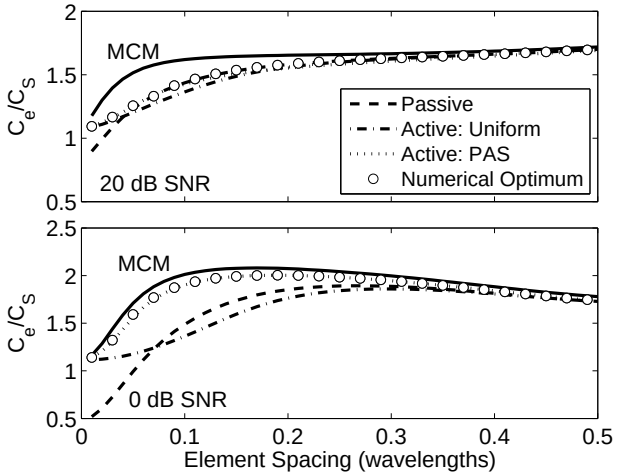

Fig. 4. Normalized average capacity as a function of element spacing for a PAS described by a single Laplacian cluster arriving on a two-element array at endfire for different matching conditions and two different SNR levels.

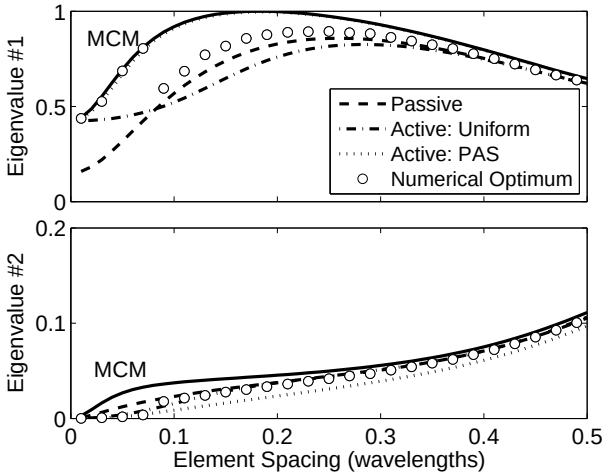

Fig. 5. Normalized eigenvalues of the covariance $\mathbf{K}_{\mathrm{s}}$ as a function of element spacing for a PAS described by a single Laplacian cluster arriving on a two-element array at endfire and for SNR = 20 dB.

Laplacian PAS is centered at $\bar{\phi} = 0°$ (endfire). Despite the simplicity of these simulations, they teach some clear principles. For example, when the SNR is low, the termination obtained by actively matching to the incident PAS is optimal. In this scenario, only one of the two possible communication modes can be efficiently used for MIMO communication, and therefore the termination that matches to the incident PAS functions as a beamformer that enhances the quality of the dominant mode. The benefit of this beamforming is less pronounced for broadside excitation, since in this case all solutions consist of identical terminations on the two antennas due to the problem symmetry, and therefore the active match offers little benefit over other terminations.

When the SNR is high, matching to the active impedance maximizes the capacity when the element spacing is small. Here, the high signal correlation creates a scenario where only one mode is useful, and therefore the termination-induced beamforming enhances the communication. As the element separation increases, however, it becomes beneficial to equalize the two modes rather than enhance one mode at the expense of the other. The termination resulting from matching to the passive impedance does not attempt to beamform for the PAS and therefore better accomplishes this mode equalization.

The relationship between beamforming gain and capacity is reinforced by examining the eigenvalues of the covariance $\mathbf{K}_{\mathrm{s}}$. Figure 5 plots these two eigenvalues, normalized so that the maximum value is unity, for the case of the PAS arriving at $\bar{\phi} = 0°$ (endfire) and for an SNR of 20 dB. These results clearly show that the active match to the PAS maximizes the dominant eigenvalue at the expense of the other, reinforcing its nature as a beamformer. The eigenvalues for the numerically optimized termination mirror this behavior for small element separation but then abruptly jump to become more equalized as the spacing increases. Despite this abrupt change in eigenvalues, the capacity of the optimized solution is smooth, showing that this change represents a transition from the optimality of beamforming enhancement of a single communication mode to the exploitation of multiple modes. The power delivered to the loads for this scenario is shown in Fig. 6, with a behavior that reinforces these concepts.

The superiority of the passive impedance match for high SNR is consistent with recent work demonstrating that this match maximizes the upper bound on the capacity when the SNR is large enough to satisfy $P_T\lambda_m/\sigma_\eta^2 \gg 1$ in each term of the capacity expression of (17) [16]. When interpreting the results in Figs. 3 and 4, it is important to recognize that even when the SNR is 20 dB, the second eigenvalue for small element spacing is so weak that this high-SNR approximation does not apply, which explains why the passive impedance match does not maximize capacity in this regime.

Figure 6 also shows the level of supergain, as measured by the effective Q-factor, for the different terminations. These results reveal that the terminations produced by MCM, numerical optimization, and active matching to the PAS yield relatively large effective Q-factors for small element separation, consistent with their nature as beamformers.

We have also characterized the array and the corresponding reference of isolated antennas numerically using the method of moments (MoM) implementation of [23] for half-wave dipoles of diameter $\lambda/400$. We find that the results and therefore our analysis closely match what we have observed using the closed-form antenna characteristics. As one example, Fig. 7 shows the capacity for two SNR levels as a function of element spacing when the PAS is uniform in azimuth. In this case, not surprisingly, the behavior for the termination for active matching to the PAS matches that obtained for the termination for active matching to a spherically uniform PAS, since the two PAS structures are the same in azimuth. This indicates that for a dipole array in this orientation, the resulting termination is relatively insensitive to the elevation structure of the PAS.

E. Three-Element Dipole Arrays

Fig. 8 plots the capacity for a SISO SNR of 0 dB for linear and triangular arrays of three dipoles, again characterized

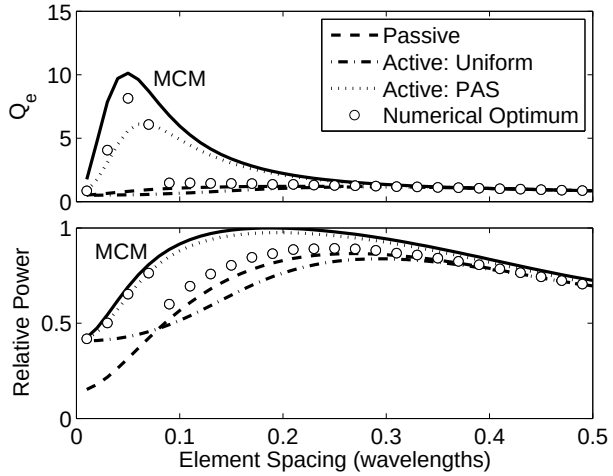

Fig. 6. Effective Q-factor and average power delivered to the loads as a function of element spacing for a PAS described by a single Laplacian cluster arriving on a two-element array at endfire and for SNR = 20 dB.

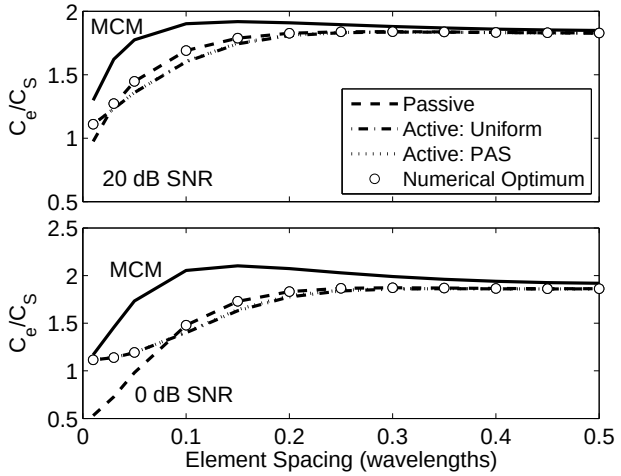

Fig. 7. Normalized average capacity as a function of element spacing for a uniform PAS for different matching conditions and two different SNR levels with the elements characterized using MoM.

using the MoM, as shown in the figure inset. The PAS is a single Laplacian cluster at $\bar{\phi} = 0^\circ$ (endfire to the linear array), and only key curves are plotted to simplify the discussion. In this case, the larger array aperture perpendicular to the cluster for the triangular array enables a higher overall capacity, while the beamforming enabled by the active PAS match provides a larger relative benefit for the linear array than the triangular array for moderate element separation.

F. Applicability to other Antennas

The framework presented here can be used to formulate uncoupled matching networks for other coupled antenna topologies. However, we can directly use the results presented here to estimate what might occur for other antennas. What complicates such a comparison is that the capacity depends on the correlation, which is a function of the multipath structure and the antenna spacing, as well as the quality of the match. Fortunately, this information is contained in the eigenvalues of the covariance matrix. Therefore, if one can find a dipole spacing for which the eigenvalues in Fig. 5 are similar to those of the target antenna, then using the capacity from Fig. 4 corresponding to the selected spacing will give an estimate of the capacity for the MIMO system using the target array.

IV. Matching for Noise Figure

The discussion on matching to maximize power transfer has provided valuable insights into the behavior of different matching topologies. However, this discussion would be incomplete without considering impedance matching for practical receivers where the front-end amplifiers represent a dominant noise source. In this situation, some amplifier noise is coupled between ports due to the antenna coupling, and the matching between the antennas and the amplifiers directly controls the front-end noise figure and system capacity.

A. Matching Implementation

The challenge of identifying an uncoupled termination that achieves minimum receiver noise figure is that it is based on a theory of optimally *mismatching* the antennas to the front-end amplifiers. In this case, rather than use the simple receiver model of Fig. 2(a), we introduce a matching network between the antennas and amplifiers using the model and theory derived in [4]. For the sake of conciseness, this analysis will not be repeated here, and we only indicate that the goal of the matching network is to transform the antenna impedance such that it appears to the amplifiers as the optimal noise figure termination with diagonal impedance matrix $\mathbf{Z}_{\rm opt}$. Naturally, this precise condition is only satisfied either for a specific incident field or for a coupled matching network.

Given the different matching techniques outlined in Section II, the challenge is to determine the mechanism for specifying the characteristics of the matching network to achieve the goal of minimum noise figure. In the context of the theory presented in [4], we have found that the following sequence of steps produces reasonable results:

1) Use the theory outlined in Section II to design the load $\mathbf{Z}_L$ that achieves maximum power transfer.
2) Given this load, assume that the active impedance seen looking into the antenna terminals is $\mathbf{Z}_{\rm act} = \mathbf{Z}_L^*$.
3) Using the theory in [4], design the uncoupled matching network that transforms this uncoupled antenna active impedance to $\mathbf{Z}_{\rm opt}$. Note that, since the theory in [4] uses the S-parameter representation, $\mathbf{Z}_{\rm act}$ must be converted to a diagonal reflection coefficient for this computation.

This approach works for the active impedance matching techniques as well as the passive impedance match. However, rather than use this approach for the active impedance match assuming a uniform PAS, we instead use the theory in [6] that presents a similar solution achieving the goal of minimum noise figure for the uniform PAS.

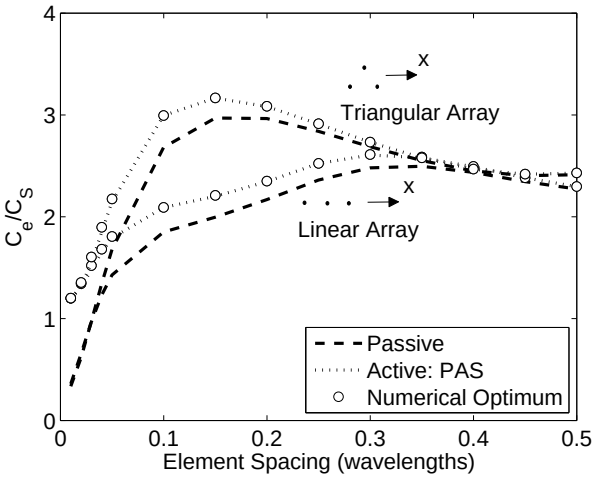

Fig. 8. Normalized average capacity as a function of element spacing for a PAS described by a single Laplacian cluster arriving at $\bar{\phi} = 0^\circ$ on linear and triangular three-element arrays characterized using MoM for SNR = 0 dB.

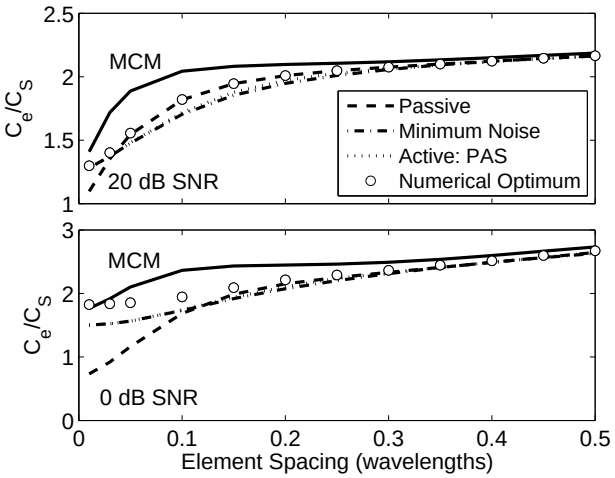

Fig. 9. Normalized average capacity as a function of element spacing for a PAS described by a single Laplacian cluster arriving on a two-element array at broadside for different matching conditions and two different SNR levels with the elements characterized using MoM.

B. Example Computation

Computations performed using this theory generally demonstrate that the basic observations and conclusions made in connection with the results presented in Section III apply to the case of optimal noise matching. As an example, consider again the two-element dipole array with the Laplacian cluster arriving at array broadside and the elements characterized using MoM. The transistors forming the amplifiers have noise parameters $R_{\rm n} = 3.5\Omega$, $Z_0 = 50\Omega$, $F_{\rm min} = 2.5$ dB, $\Gamma_{\rm opt} = 0.475\angle 166^\circ$ (optimal reflection coefficient), and an input impedance of 50Ω (see [4] for a detailed discussion on how these are used in the design and simulations).

Figure 9 plots the capacity resulting from this analysis for two different values of SISO SNR, where the "Minimum Noise" match is that obtained from [6]. As can be seen, under this procedure, the conclusions for high SNR are similar to those obtained during the analysis of matching for maximum power transfer. Specifically, when the SNR is high, matching to the active impedance (including the solution from [6]) leads to optimal performance only for high coupling, while matching to the passive impedance is optimal elsewhere.

However, when the SNR is low, the numerically optimum solution outperforms all other uncoupled solutions for high antenna coupling. Closer investigation of this case reveals that, despite the problem symmetry that suggests identical matching on the antenna ports, the numerical solution provides asymmetric matching to achieve these results. In fact, when the optimization is constrained to produce symmetric matching, the numerically-optimized solution follows the analytical curves as observed in all other capacity plots in this paper. This means that at low SNR, degrading the quality of one output port to enhance the quality on the other provides benefit. We also point out that the port selected to achieve improved performance is arbitrary. Given the symmetric nature of this problem, it is currently unclear as to how to develop a closed-form matching strategy to achieve this behavior. However, it is important to recognize that this case of high coupling and low SNR is impractical for most realistic communication scenarios.

V. Conclusions

This paper uses a common framework to develop and analyze uncoupled impedance matching for coupled array antennas. Specifically, it discusses matching to the array active impedance for deterministic and stochastically-specified electromagnetic fields, and shows that such active matching in effect creates a beamformer that maximizes received power. It also discusses a previously-proposed technique for matching to the antenna passive impedance, also referred to as input impedance matching, known to be optimal in certain circumstances. Simulation results of MIMO capacity using different propagation environments demonstrate that for low SNR or high coupling, active matching outperforms passive matching due to the associated beamforming gains. However, for moderate coupling or high SNR, passive impedance matching enables better use of the multiple communication modes. The discussion concludes by demonstrating the application of the matching techniques for minimizing the system noise figure.

References

[1] H. A. Haus and R. B. Adler, *Circuit Theory of Linear Noisy Networks*. New York: Wiley, 1959.

[2] J. B. Andersen and H. H. Rasmussen, "Decoupling and descattering networks for antennas," *IEEE Trans. Antennas Propag.*, vol. AP-24, no. 6, pp. 841–846, Nov. 1976.

[3] J. W. Wallace and M. A. Jensen, "Mutual coupling in MIMO wireless systems: A rigorous network theory analysis," *IEEE Trans. Wireless Commun.*, vol. 3, pp. 1317–1325, Jul. 2004.

[4] M. L. Morris and M. A. Jensen, "Network model for MIMO systems with coupled antennas and noisy amplifiers," *IEEE Trans. Antennas Propag.*, vol. 53, pp. 545–552, Jan. 2005.

[5] K. F. Warnick and M. A. Jensen, "Effects of mutual coupling on interference mitigation with a focal plane array," *IEEE Trans. Antennas Propag.*, vol. 53, pp. 2490–2498, Aug. 2005.

[6] K. Warnick, E. Woestenburg, L. Belostotski, and P. Russer, "Minimizing the noise penalty due to mutual coupling for a receiving array," *IEEE Trans. Antennas Propag.*, vol. 57, no. 6, pp. 1634–1644, Jun. 2009.

[7] B. K. Lau, J. B. Andersen, G. Kristensson, and A. Molisch, "Impact of matching network on bandwidth of compact antenna arrays," *IEEE Trans. Antennas Propag.*, vol. 54, no. 11, pp. 3225–3238, Nov. 2006.
[8] P. W. Hannan, "The element-gain paradox for a phased-array antenna," *IEEE Trans. Antennas Propag.*, vol. 12, no. 4, pp. 423–433, Jul. 1964.
[9] D. Schaubert, A. Boryssenko, A. van Ardenne, J. Bij de Vaate, and C. Craeye, "The square kilometer array (SKA) antenna," in *Proc. 2003 IEEE Intl. Symps on Phased Array Systems and Technology*, Boston, MA, Oct. 14-17, 2003, pp. 351–358.
[10] C. Craeye, B. Parvais, and X. Dardenne, "MoM simulation of signal-to-noise patterns in infinite and finite receiving antenna arrays," *IEEE Trans. Antennas Propag.*, vol. 52, no. 12, pp. 3245–3256, Dec. 2004.
[11] J. B. Andersen and B. K. Lau, "On closely coupled dipoles in a random field," *IEEE Antennas Wireless Propagat. Lett.*, vol. 5, pp. 73–75, 2006.
[12] B. K. Lau, J. B. Andersen, G. Kristensson, and A. F. Molisch, "Antenna matching for capacity maximization in compact MIMO systems," in *Proc. 3rd Int. Symp. Wireless Commun. Syst.*, Valencia, Spain, Sep. 2006, pp. 253–257.
[13] W. Geyi, "Derivation of equivalent circuits for receiving antenna," *IEEE Trans. Antennas Propag.*, vol. 52, no. 6, pp. 1620–1624, Jun. 2004.
[14] B. T. Quist and M. A. Jensen, "Optimal antenna radiation characteristics for diversity and MIMO systems," *IEEE Trans. Antennas Propag.*, vol. 57, no. 11, pp. 3474–3481, Nov. 2009.
[15] R. Vaughan and J. B. Andersen, "Antenna diversity in mobile communications," *IEEE Trans. Veh. Technol.*, vol. 36, no. 4, pp. 149–172, Nov. 1987.
[16] Y. Fei, Y. Fan, B. K. Lau, and J. Thompson, "Optimal single-port matching impedance for capacity maximization in compact MIMO arrays," *IEEE Trans. Antennas Propag.*, vol. 56, no. 11, pp. 3566–3575, Nov. 2008.
[17] M. Uzsoky and L. Solymar, "Theory of super-directive linear antennas," *Acta Physica Hungarica*, vol. 6, no. 2, pp. 185–205, 1956.
[18] Y. T. Lo, S. W. Lee, and Q. H. Lee, "Optimization of directivity and signal-to-noise ratio of an arbitrary antenna array," *Proc. IEEE*, vol. 54, pp. 1033–1045, Aug. 1966.
[19] N. W. Bikhazi and M. A. Jensen, "The relationship between antenna loss and superdirectivity in MIMO systems," *IEEE Trans. Wireless Commun.*, vol. 6, no. 5, pp. 1796–1802, May 2007.
[20] H. Özcelik, M. Herdin, W. Weichselberger, J. Wallace, and E. Bonek, "Deficiencies of 'Kronecker' MIMO radio channel model," *Electronics Letters*, vol. 39, pp. 1209–1210, Aug. 7 2003.
[21] L. Schumacher, K. I. Pedersen, and P. E. Mogensen, "From antenna spacings to theoretical capacities - guidelines for simulating MIMO systems," in *Proc. 2002 IEEE 13th Intl. Symp. on Personal, Indoor and Mobile Radio Comm.*, vol. 2, Lisboa, Portugal, Sep. 15-18, 2002, pp. 587–592.
[22] C. A. Balanis, *Antenna Theory: Analysis and Design*. Wiley, 1997.
[23] S. M. Makarov, *Antenna and EM Modeling with MATLAB*. New York: John Wiley and Sons, 2002.

PLACE PHOTO HERE

Michael A. Jensen (S'93, M'95, SM'01, F'08) received the B.S. (summa cum laude) and M.S. degrees in Electrical Engineering from Brigham Young University (BYU) in 1990 and 1991, respectively, and the Ph.D. in Electrical Engineering from the University of California, Los Angeles in 1994. Since 1994, he has been at the Electrical and Computer Engineering Department at BYU where he is currently a Professor and Department Chair. His research interests include antennas and propagation for communications, microwave circuit design, and multi-antenna signal processing.

Dr. Jensen currently chairs the Joint Meetings Committee for the IEEE Antennas and Propagation Society and is an Associate Editor for the IEEE ANTENNAS AND WIRELESS PROPAGATION LETTERS. He has been an Associate Editor for the IEEE TRANSACTIONS ON ANTENNAS AND PROPAGATION, a member of the society AdCom, and Co-Chair and Technical Program Chair for several symposia. He was awarded the H. A. Wheeler paper award in the IEEE TRANSACTIONS ON ANTENNAS AND PROPAGATION in 2002.

PLACE PHOTO HERE

Buon Kiong Lau (S'00, M'03, SM'07) received the B.E. degree (with honors) from the University of Western Australia, Crawley and the Ph.D. degree from Curtin University of Technology, Perth, Australia, in 1998 and 2003, respectively, both in electrical engineering.

During 2000-2001, he took a year off from his Ph.D. studies to work as a Research Engineer with Ericsson Research, Kista, Sweden. From 2003 to 2004, he was a Guest Research Fellow at the Department of Signal Processing, Blekinge Institute of Technology, Sweden. In 2004, he was appointed a Research Fellow in the Department of Electrical and Information Technology, Lund University, Sweden, where he is now an Assistant Professor. During 2003, 2005 and 2007, he was also a Visiting Researcher at the Department of Applied Mathematics, Hong Kong Polytechnic University, China, the Laboratory for Information and Decision Systems, Massachusetts Institute of Technology, and Takada Laboratory, Tokyo Institute of Technology, Japan, respectively. His research interests include array signal processing, wireless communication systems, and antennas and propagation.

Dr. Lau is an active participant of EU COST Action 2100, where he is the Co-Chair of Subworking Group 2.2 on Compact Antenna Systems for Terminal.